Published as: *Cell*. 2013 October 10; 155(2): 296–307.

An extracellular adhesion molecule complex patterns dendritic branching and morphogenesis

Xintong Dong, **Oliver W. Liu**, **Audrey S. Howell**, and **Kang Shen**
Howard Hughes Medical Institute, Department of Biology, Stanford University, 385 Serra Mall, California 94305, USA

Summary

Robust dendrite morphogenesis is a critical step in the development of reproducible neural circuits. However, little is known about the extracellular cues that pattern complex dendrite morphologies. In the model nematode *C. elegans*, the sensory neuron PVD establishes stereotypical, highly-branched dendrite morphology. Here, we report the identification of a tripartite ligand-receptor complex of membrane adhesion molecules that is both necessary and sufficient to instruct spatially restricted growth and branching of PVD dendrites. The ligand complex SAX-7/L1CAM and MNR-1 function at defined locations in the surrounding hypodermal tissue, while DMA-1 acts as the cognate receptor on PVD. Mutations in this complex lead to dramatic defects in the formation, stabilization, and organization of the dendritic arbor. Ectopic expression of SAX-7 and MNR-1 generates a predictable, unnaturally patterned dendritic tree in a DMA-1 dependent manner. Both *in vivo* and *in vitro* experiments indicate that all three molecules are needed for interaction.

Introduction

The establishment of a complex, type-specific dendrite morphology is crucial for many neurons to receive the appropriate inputs from their receptive fields and to properly function within a neural circuit. As with axon morphogenesis, the development of dendrites must be precisely regulated to achieve the appropriate structure. However, the immense complexity of dendrite morphology has made it far more challenging to study than the pathfinding of a single axon (Jan and Jan, 2010).

Dendrites receive extrinsic cues from the adjacent environment to guide their spatially regulated growth and branching. Several molecules originally identified as axon guidance signals also play important roles in directing dendritic morphogenesis. Cortical pyramidal neurons extend their apical dendrites towards the pial surface in response to the diffusible chemoattractant Semaphorin 3A (Polleux et al., 2000). In the mammalian retina, dendritic arbors of amacrine cells and retinal ganglion cells (RGCs) are strictly organized in defined laminae in the inner plexiform layer (IPL) (Sanes and Zipursky, 2010). A number of neuronal homotypic adhesion molecules including Sdk1, Sdk2, Dscam, DscamL and Cntn2 restrict arbors to specific sublaminae (Yamagata and Sanes, 2008, 2012). Repulsive mechanisms mediated by a transmembrane semaphorin Sema6A and its receptor PlexA4 are

Contact (corresponding author) Kang Shen (kangshen@stanford.edu).

also required to restrict layer specific arbor targeting (Matsuoka et al., 2012). Similarly, dendrites of projection neurons in the *Drosophila* olfactory system utilize graded expression of Semaphorin 1A and the differentially-expressed leucine rich repeat (LRR) protein Caps for precise glomeruli targeting (Hong et al., 2009; Komiyama et al., 2007). Dendrites can also avoid sister branches from the same neuron while co-existing with the arbors of their neighboring neurons. This self-avoidance phenomenon has been elegantly explained by the function of two classes of highly diversified, contact-dependent repulsive molecules, DSCAMs in *Drosophila* and protocadherins in vertebrates (Lefebvre et al., 2012; Matthews et al., 2007; Schmucker et al., 2000; Soba et al., 2007; Wojtowicz et al., 2004; Wojtowicz et al., 2007).

However, our current understanding of spatial dendritic patterning is not yet complete. A key component still missing from the puzzle is the interaction between dendrites and their growth substrate. It has been shown that confinement of the dendritic arbors to a precise 2D surface by the growth substrate is necessary for further refinement of receptive fields through dendro-dendritic interactions (Han et al., 2012; Kim et al., 2012; Yasunaga et al., 2010). However, the molecular identities of the signals on the growth substrate and corresponding neuronal receptors that instruct the growth, directionality, and branching of dendrites remain largely elusive.

The multi-dendritic PVD neurons in the nematode *Caenorhabditis elegans* provide us with a unique opportunity to study these questions. PVDs grow elaborate, highly-branched and well-organized dendritic arbors (Smith et al., 2010) (Fig. 1A). The cell bodies of the two PVD neurons, PVDL and PVDR, are derived post-embryonically during the mid-L2 larval stage along the lateral midlines underneath the hypodermal cells on each side of the worm. During L2, each cell extends two 1° dendrites (anteriorly and posteriorly) and one ventrally oriented axon. By late L2/early L3, 2° branches form perpendicular to the 1° branches. When the 2° branches reach the lateral borders of the outer body wall muscles, most 2° branches make 90° turns and then form collateral 3° branches (Smith et al., 2010). All 3° PVD branches extend along the same line that largely colocalizes with the sublateral nerve cords. Dendrite morphogenesis is completed in early L4 stage after 4° branches have sprouted from the 3° branches to form a network of candelabra - shaped processes. This structure follows general dendritic organization principles such as self-avoidance (Smith et al., 2010). Understanding how the PVD dendrites make decisions about growth and branching at stereotyped times and locations will provide insights on the genetic components involved in the regulation of dendrite development.

Several reports have been published on the intrinsic molecules that are involved in shaping and maintaining PVD morphology. These include transcription factors (Smith et al., 2013; Smith et al., 2010), cell trafficking components (Aguirre-Chen et al., 2011), a membrane fusion protein (Oren-Suissa et al., 2010), and factors involved in dendrite self-avoidance (Smith et al., 2012). Our lab previously identified a transmembrane LRR protein, DMA-1, which is required cell-autonomously in PVD for the formation of dendritic branches (Liu and Shen, 2012). DMA-1 is expressed most prominently in the PVDs and another pair of multi-dendritic sensory neurons, the FLP head neurons. Loss-of-function mutants of *dma-1* show severely defective dendritic arbors, whereas overexpression causes overbranching. We reasoned that DMA-1 may be the neuronal receptor that signals the development of PVD dendritic branches but the extrinsic ligands that instruct the precise patterning of the dendritic trees remain to be identified.

In this paper, we report the identification and characterization of a tripartite receptor-ligand complex of cell surface proteins that plays an instructive role in directing the formation and growth of dendritic branches. We provide both genetic and biochemical evidence that

SAX-7, a homolog of vertebrate L1 cell adhesion molecules (L1CAM), and its co-ligand, MNR-1, form pre-patterned signals in the skin hypodermal cells to direct dendrite morphogenesis through the neuronal receptor, DMA-1.

Results

Mutations in *sax-7*, *mnr-1*, and *dma-1* cause defects in PVD dendritic morphology

We visualized the PVD neurons using a membrane-GFP marker expressed under the control of a cell specific promoter (*ser2prom3*: *myrGFP*) (Fig. 1A) and conducted both candidate and forward genetic screens for mutations that altered PVD dendritic morphology. A loss-of-function mutant of a conserved immunoglobulin (Ig) superfamily cell adhesion molecule, SAX-7/L1CAM, showed a disorganized PVD dendritic structure. Instead of growing orthogonally to the 1° branches, the 2° branches in *sax-7* mutants were misdirected and frequently overlapped (Fig. 1B). In addition, the *sax-7* mutants completely lacked the candelabra structures formed by the 3° and 4° branches. Although some 2° branches could successfully reach the sublateral line where the 3° branches normally form, they failed to generate the stereotypical “T”-shaped branches through collateral formation, and instead only formed an “L” shaped turn or even remained as an “I”-shaped 2° neurite, suggestive of a branching defect (Fig. 1B, arrows, Fig. 1E). Since the branches largely overlapped and were difficult to quantify at the adult stage, we quantified the 3° branch formation phenotype in early L3 worms (36-38 hour after egg-laying) when all of the 3° branches have fully developed in wild-type worms but the 4° branches have not started to grow. Using pan-neuronally expressed mCherry as landmark, we counted the total number of 2° branches that grew to the sublateral line where 3° branches normally form and the fraction of branches that failed to form a “T” shape at this developmental stage. In wild-type worms, more than 80% of “L” shaped branches formed collaterals, while dendrites in the *sax-7(nj48)* mutants completely failed to do so, suggesting that SAX-7/L1CAM is required for the initiation or maintenance of the 3° branches (Fig. 1E, F).

Through an unbiased forward genetic screen, we found that a complementation group defined by the mutations *wy758*, *wy771* and *wy776* showed dendrite morphology phenotypes that were indistinguishable from those of the *sax-7* mutants (Fig. 1C, F). In all animals, 3° and 4° branches were completely absent, and the 2° branches were disorganized. Using SNP mapping, sequencing, and transgene rescue experiments, we localized the responsible mutations to the novel gene W01F3.1, now named *menorin*, or *mnr-1*. *mnr-1* encodes a putative type I transmembrane protein that is conserved in vertebrates (Fig. S1). *mnr-1(wy758)* has a nonsense G-to-A point mutation that presumably truncates two thirds of the protein and is likely to be a null allele.

We have previously shown that a leucine-rich repeat transmembrane protein, DMA-1, is required for the development of candelabras. *dma-1* mutants have a greatly reduced number of 2° branches (Liu and Shen, 2012), a phenotype distinct from that of *sax-7* and *mnr-1*. However, close examination of the *dma-1* mutants revealed that many of the remaining branches, mostly those associated with motor neuron commissures, were able to reach the sublateral line where the 3° branches normally form (36.2±13.0% of all branches, N=20). These branches still completely failed to generate any 3° branches and displayed only “L” or “I” shaped structures (Fig. 1D, F). This aspect of the phenotype is very similar to that of *sax-7* and *mnr-1* mutants, suggesting that these three membrane molecules might work together to regulate development of the PVD dendritic branches. We used a series of experiments to test this hypothesis.

SAX-7 and MNR-1 function in the hypodermal cell as a pre-patterned cue

To understand where SAX-7 and MNR-1 function to pattern PVD dendrites, we first examined the endogenous expression pattern of both genes by introducing C-terminal GFP tags followed by SL2-mCherry into fosmids containing the entire genomic loci (Tursun et al., 2009). SL2 sequences are trans-splicing sites for mRNA, similar to the IRES sites in vertebrate systems (Zorio et al., 1994). These constructs revealed the cellular expression of the genes and pinpointed the subcellular localization of protein products. The mCherry signal revealed that SAX-7 was expressed in the hypodermal cells and in many neurons, but not in PVD (Fig. 2D). Within the hypodermal cell, SAX-7: :GFP showed specific localization to two sublateral stripes and the hypodermal-seam cell junctions (Fig. 2C, arrows). In contrast, MNR-1 was exclusively expressed in the hypodermis (Fig. 2H) and did not exhibit similar subcellular localization (Fig. 2G).

In *C. elegans*, the PVD dendritic processes are positioned in a narrow space between the hypodermis and the internal organs, similar to mammalian somatosensory neurons (Albeg et al., 2011). Since neither SAX-7 nor MNR-1 were expressed in the PVD neurons but were instead found in the PVD growth substrate (the hypodermal cell) we hypothesized that they might function as extrinsic signals to pattern the PVD dendrites. To definitively test which cells require SAX-7 and MNR-1, we expressed SAX-7 or MNR-1 using tissue-specific promoters in their respective mutant backgrounds. Expressing SAX-7 in the hypodermal cells using the *dpy-7* promoter completely rescued the *sax-7* phenotype (Fig. 2B), while expression of SAX-7 in the PVD neuron or muscles showed no rescue, suggesting that SAX-7 functions non-cell-autonomously in the surrounding hypodermal cell (Fig. 2I). Similarly, we found that expression of MNR-1 in the hypodermal cells alone also rescued the *wy758* phenotype (Fig. 2F), while expression in the PVD neuron resulted in no rescue (Fig. 2J). These results are consistent with the expression analysis and suggest that both SAX-7 and MNR-1 function in the hypodermal cell to pattern the PVD dendrites.

Since *sax-7* and *mnr-1* mutants showed identical phenotypes and are both transmembrane proteins functioning in the hypodermal cell, we considered the possibility that they function as co-ligands. Consistent with this hypothesis, *sax-7; mnr-1* double mutants showed an identical phenotypes to *sax-7* and *mnr-1* single mutants, without any apparent enhancement or suppression (Fig. 2K). The two genes thus function in the same genetic pathway.

The requirement of SAX-7 in the hypodermal cell prompted us to examine its subcellular localization in more detail. We expressed a functional SAX-7: :YFP fusion protein in the hypodermal cell under the *dpy-7* promoter. We found that SAX-7: :YFP was enriched at the hypodermal-seam cell junctions and also formed two longitudinal sublateral stripes on each side of the worm (Fig. 3B), similar to SAX-7 under the control of its own promoter (Fig. 2C). These stripes are especially interesting because they are located along the edge of outer body wall muscles where the PVD 3° branches are aligned (Albeg et al., 2011). Since the PVD dendrites have been previously reported to associate with other neurons including those forming the sublateral nerve cord (Smith et al., 2010), we sought to tease apart the relationship between PVD, SAX-7, and other neurons in the sublateral cords by co-expressing mCherry in PVD (Fig. 3A), SAX-7: :YFP in the hypodermis (Fig. 3B), and CFP in all neurons (Fig. 3C). In the anterior half of the worm, it was apparent that the PVD 3° branches co-localized with the sublaterally-enriched SAX-7 line, but not with other neuronal processes (Fig. 3D). Expression and localization of SAX-7 was observed early in development during the L1 and early L2 stages, long before the formation of PVD branches (Fig. S2A, B). The localization of SAX-7 was normal in *mnr-1(wy758)* mutants, where PVD dendritic organization was completely lost (Fig. S2C-E). SAX-7 localization and PVD 3° branch structure were also unaffected in an axon guidance mutant, *mig-10(ct41)*, in which a small portion of the sublateral nerve cord is missing (data not shown). Thus, hypodermal

SAX-7 was expressed and localized independent of the presence of PVD branches or the sublateral neurons. Together, these observations support the hypothesis that the sublaterally-enriched SAX-7, together with MNR-1, functions as a pre-patterned cue that instructs the growth of PVD dendrites.

Developmental analysis of PVD dendritic morphogenesis with time-lapse imaging

The absence of 3° branches in *sax-7*, *mnr-1*, and *dma-1* worms could arise from a failure in 3° branch initiation, stabilization, or both. To further understand the phenotypes of *sax-7*, *mnr-1* and *dma-1*, we performed time-lapse analysis on these mutants to observe how the wild-type and mutant dendritic arbors are established during development. We observed PVD branch formation relative to the sublateral nerve cord using worms expressing *ser2prom3*: :*myr-gfp* and P*rab-3*: :*mCherry*. Consistent with previous reports, the majority of "T"-shaped 3° branches arose via collateral formation from "L"s in wild-type animals (Smith et al., 2010). However, we also observed that a subset of "T"s appeared to form through direct bifurcation of the secondary branches (10%, n=30 branches). To understand the mutant defects, we quantified transitions between the different growth stages of the dendrites. In wild-type animals, nearly half of all of the branches that reached the sublateral line went on to eventually form a "T" (49.2%, n=61 branches) (Fig. 4A and Movie S1). Of those branches that formed an "L" at the sublateral line, the majority (57.4%, n=47) transitioned to "T"s during filming (18% of branches that reached the sublateral cord remained "I"s during the course of filming, n=61). Significantly fewer of the branches that reached the sublateral cord in *sax-7*, *mnr-1* and *dma-1* mutants went on to initiate a "T" (22.9%, n=48; 18.8%, n=32; and 11.1%, n=36, respectively; Fig. 4A and Movies S2-S4), suggesting that these three molecules play an important role in collateral branch formation along the 3° branch line.

Once a "T" had formed, the 3° branch exhibited dynamic growth and retraction. In wild-type animals, the majority of the "T"-shaped branches were stabilized over the course of filming, however 43.3% (n=30) of the "T"s retracted to an "L" or "I" (Fig. 4B and Movie S1). In *sax-7*, *mnr-1* and *dma-1* mutants, nearly all the "T" s retracted to an "L" or "I" (81.8%, n=11; 100%, n=6; 100%, n=4, respectively, Fig. 4B and Movies S2-S4), suggestive of a failure to maintain the 3° branch. However, due to the branch initiation defects in these mutants, the number of "T"s we could successfully image was low, therefore the difference in "T" retraction rate between wild-type and mutant worms did not reach statistical significance (Fig. 4B).

SAX-7, MNR-1, and DMA-1 do appear to contribute to overall branch stability, however. A majority of branches that reached the sublateral line in these three mutant worms retracted back towards the primary dendrite, often completely disappearing, even after "L" or "T" initiation (54.2%, n=48; 68.8%, n=32; and 83.3%, n=36, respectively; Fig. 4C). Such retractions of branches that reached the sublateral line were significantly less frequent in wild-type worms (13.1%, n=61; Fig. 4C) suggesting that the mutants do exhibit a defect in branch stability. Additionally, although *dma-1* mutant worms had an overall reduced number of 2° branches (Liu and Shen, 2012), we observed frequent initiation and retraction of branches during filming (Movie S4) suggesting that the lack of 2° branches in *dma-1* mutants is due, in part, to reduced branch stabilization rather than a loss of 2° branch initiation. Taken together, our time-lapse analysis of the dynamic growth of dendritic branches showed that the *sax-7*, *mnr-1* and *dma-1* mutants exhibited markedly similar phenotypes: they have a reduced ability to initiate 3° branches and have compromised branch stabilization. These two developmental phenotypes caused the 3° branches to be completely absent in all three mutants at later stages in development.

Ectopic expression of SAX-7 and MNR-1 alters PVD dendritic morphology

To further test whether SAX-7 and MNR-1 play instructive roles in directing the development of PVD dendrites, we expressed these proteins ectopically in various tissues to determine whether they could alter PVD morphology. We first expressed SAX-7 in the seam cells using the *nhr-81* promoter. Seam cells are egg-shaped specialized epithelial cells that are arranged in longitudinal rows on the left and right sides of the worm body (Sulston and Horvitz, 1977). They penetrate the hypodermis and make contact with the PVD dendrites at their thickest parts where the cell body is located, but are buried in the hypodermal cell on their narrow ends. Ectopic seam cell expression of SAX-7 in *sax-7(nj48)* single mutants resulted in a striking, fully penetrant gain-of-function (gof) phenotype in which all PVD dendrites were restricted around the seam cells (Fig. 5A). Such gof phenotype was completely abolished in the mutant background of *mnr-1(wy758)*. The branches displayed a phenotype identical to the *mnr-1* single mutants with no sign of following the seam cells (Fig. 5B, D). We quantified the phenotype by counting the number of dendrites that grew outside the estimated positions of the seam cells in each worm. PVD morphology was indistinguishable between *mnr-1* mutant worms that carried the SAX-7 gof transgene and those that did not (Fig. 5D). However, when we put MNR-1 back into the hypodermal cells using the *dpy-7* promoter, the gof phenotype could be fully rescued (Fig. 5D).

These results show that MNR-1 is required for SAX-7 to exert its instructive function, consistent with our hypothesis that the two molecules function as co-ligands. However, how can hypodermal MNR-1 assist the function of seam cell SAX-7? One possibility is that MNR-1 can function as a secreted molecule. We tested this hypothesis by expressing MNR-1 without its predicted C-terminal transmembrane domain, which should cause it to be secreted. Expressing this construct in the *mnr-1(wy758)* mutant resulted in a partial rescue. Many dendrites were able to recognize the sublateral SAX-7 cue and form “T”-shaped tertiary structures, but they failed to further form quaternary branches (Fig. S3A). This result indicates that secreted MNR-1 is partially functional. To directly test if MNR-1 can be secreted, we tagged full-length MNR-1 on its extracellular side with mCherry and expressed it under the *dpy-7* promoter. Fluorescence could be detected in the coelomocytes, which are phagocytic cells that uptake and concentrate extracellular materials from the body cavity, similar to vertebrate macrophages (Fig. S3B) (Sulston and Horvitz, 1977). This supports the model that at least some MNR-1 is secreted.

In further experiments, we expressed SAX-7 and MNR-1 together in mechanosensory neurons, including the PLMs and ALMs, using the *mec-17* promoter in *sax-7; mnr-1* double mutants. We chose PLMs and ALMs because they are part of the sublateral nerve cords that largely colocalize with the hypodermal SAX-7 and PVD 3° branches in the posterior half of the animal. If the pre-patterned SAX-7 and MNR-1 are indeed instructing the formation of 3° branches in wild-type animals, then expression of SAX-7 and MNR-1 in part of the sublateral nerve cords should partially rescue the 3° branching phenotype of the mutants. This is indeed what we observed. As shown in Figure 6A-C, 2° PVD branches that reached the SAX-7- and MNR-1-expressing PLM and ALM neurons formed “T”-shaped collateral 3° branches (Fig. 6B, arrowheads). We quantified the total number of 2° branches that reached the SAX-7- and MNR-1-expressing PLMs and ALMs and observed significant rescue of the “T” formation phenotype (Fig. 6F). Instead of being nearly absent in the mutants, “T”s were formed by about 50% of dendrites that made contact with the SAX-7- and MNR-1-expressing PLM or ALM neurons (Fig. 6F). We also consistently observed abnormally long PVD dendrites that completely followed the PLM or ALM processes (Fig. 6B, arrows), supporting the hypothesis that SAX-7 and MNR-1 together form a preferred substrate on which PVD branches can form and grow. When expressed independently, P*mec-17*: *sax-7* by itself produced a weaker, yet significant gof phenotype in *sax-7* single

mutants, with some PVD dendrites forming "T"'s on the PLM and ALM neurons. This effect was fully abolished in the *mnr-1* single and *sax-7; mnr-1* double mutants, consistent with the notion that MNR-1 can be partially secreted from the hypodermal cell and is necessary for SAX-7 to exert its function in directing PVD dendrites. On the other hand, expressing MNR-1 in the sublateral neurons of *mnr-1* single mutants produced an equally strong gof phenotype as expressing both SAX-7 and MNR-1 in the *sax-7; mnr-1* double mutants, consistent with our observation of endogenous SAX-7 expression in these neurons (Fig. 2C, arrowheads). This was fully abolished in *sax-7* single or *sax-7; mnr-1* double mutants (Fig. 6F). These results strongly support the model that SAX-7 and MNR-1 must function together as co-ligands to instruct morphogenesis of the PVD dendrites and that MNR-1 can be partially secreted.

We also expressed SAX-7 and MNR-1 in the D-type motor neurons using the *unc-47* promoter. The DDs and VDs form ventral-dorsal commissures that PVD 2° branches sometimes fasciculate with (Smith et al., 2010). Having SAX-7 and MNR-1 in the commissures significantly reduced the number of 2° branches growing in the wrong directions. Most 2° branches instead followed the commissures expressing SAX-7 and MNR-1 and grew symmetrically towards both the dorsal and ventral sides. Instead of stopping at the sublateral lines where they normally turn and form 3° branches, the dendrites following the SAX-7- and MNR-1-containing commissures extended all the way to the ventral and dorsal nerve cords (Fig. 6D, arrows). We quantified this phenotype by counting the percentage of 2° branches that crossed the sublateral nerve cords and found that 70% of branches did so in the worms with the transgene (Fig. 6G). These results show that SAX-7 and MNR-1 form a preferred substrate that can stimulate the branching and growth of PVD dendrites. We expressed SAX-7 and MNR-1 in both PLM, ALM as well as D-type motor neurons and found that almost all PVD dendrites followed the neuronal processes that ectopically expressed these proteins (Fig. 6E). Thus, we can reconstruct the PVD dendritic structure simply by ectopically expressing these instructive adhesion molecules as guidance cues, and we can conclude that the SAX-7/MNR-1 complex is sufficient to direct PVD dendrite growth.

DMA-1 is the neuronal receptor for SAX-7 and MNR-1

We have reported previously that mutation of a neuronal LRR gene, *dma-1*, causes severe defects in PVD 3° branches (Fig. 1D), so we considered the possibility that DMA-1 may be the neuronal receptor for hypodermal SAX-7 and MNR-1. DMA-1 functions autonomously in the PVD neuron (Liu and Shen, 2012). If DMA-1 is the receptor in the neuron and is responsible for responding to the SAX-7 and MNR-1 signal, then loss of DMA-1 should completely abolish all gof phenotypes produced by SAX-7 and MNR-1 ectopic expression. This was indeed the case. We crossed the integrated seam cell SAX-7 overexpression transgene with *dma-1(wy686)* and found that the branches failed to follow the ectopic SAX-7 signal. Instead of wrapping around the seam cells, dendrites in the *dma-1(wy686)* mutants extended towards the sublateral cords, as if the ectopic SAX-7 did not exist (Fig. 5C, D). Similarly, dendrites in the *dma-1* mutants did not respond to ectopically expressed SAX-7 and MNR-1 in PLM and ALM. Instead of being modified by the SAX-7 and MNR-1 ectopic expression transgene, dendrite morphology in these worms was indistinguishable from all other *dma-1(wy686)* mutant worms and no rescue was observed for the 3° branching phenotype (Fig. 6F, Fig. S4). To further explore these genetic interactions, we made *dma-1(wy686); sax-7(nj48)* (data not shown), *dma-1(wy686); mnr-1(wy758)* double mutants and *dma-1(wy686); sax-7(nj48); mnr-1(wy758)* triple mutants (Fig. S5A, B) and examined their PVD dendritic phenotypes. PVD morphology in all these mutants was indistinguishable from that of *dma-1* single mutants. This is consistent with the idea that SAX-7 and MNR-1 function as the upstream binding partners of DMA-1. Overexpression of

DMA-1 in PVD causes a severe overbranching phenotype (Fig. S5C) (Liu and Shen, 2012). However, in *sax-7* or *mnr-1* mutants carrying the DMA-1 overexpression transgene, PVD morphology was indistinguishable from *sax-7* or *mnr-1* single mutants (Fig. S5D, E). Together, these results indicate that DMA-1 may be the receptor for SAX-7 and MNR-1.

DMA-1 physically interacts with the SAX-7/MNR-1 ligand complex

As the genetic evidence strongly suggested that DMA-1 could be the neuronal receptor for SAX-7 and MNR-1, we tested whether DMA-1 physically interacts with SAX-7 and MNR-1 *in vitro* to form a receptor-ligand complex using a *Drosophila* S2 cell aggregation assay (Zorio et al., 1994). We transfected S2 cells with C-terminal GFP-tagged SAX-7, MNR-1 or both, and mixed them with cells expressing RFP-tagged DMA-1. Strong aggregation was observed only when cells co-transfected with both SAX-7: :GFP and MNR-1: :GFP were mixed with cells expressing DMA-1: :RFP (Fig. 7C). Little aggregation was observed in all other groups including ones in which cells expressing only SAX-7: :GFP or MNR-1: :GFP individually were mixed with DMA-1: :RFP cells (Fig. 7A-D). This argues strongly that SAX-7 and MNR-1 form a co-ligand complex in *cis* and interact with DMA-1 in an in *trans* fashion.

We also performed co-immunoprecipitation (co-IP) experiments to test direct physical interaction among these three molecules. Cells were transformed with HA-tagged SAX-7, myc-tagged DMA-1 extracellular domain and FLAG-tagged MNR-1. Again, DMA-1 and MNR-1 could only be co-precipitated when lysates of SAX-7: :HA, MNR-1: :FLAG co-transfected cells were mixed with DMA-1: :myc lysate and anti-HA beads (Fig. 7E).

The FnIII but not Ig domains of SAX-7 are required for tripartite binding

All previously reported functions of SAX-7 require homotypic interaction between its first two Ig domains (Pocock et al., 2008; Sasakura et al., 2005) whereas the fibronectin III (FnIII) domains are not necessary. We conducted structure-function analysis on SAX-7 to test whether the same domains are required for binding in the SAX-7/MNR-1/DMA-1 tripartite complex. To our surprise, the FnIII domains were both necessary and sufficient to perform the functions of SAX-7 described in this study. Truncation constructs of SAX-7 without the first one, first two or even all four Ig domains were all able to fully rescue the *sax-7* mutant phenotype of PVD when expressed in the hypodermal cell using the *dpy-7* promoter (Fig. S6A, B). Conversely, deleting all five FnIII domains completely abolished its ability to rescue (Fig. S6A, C). The same construct has been shown to be sufficient to rescue the axon integration and cell positioning phenotypes of *sax-7* mutants (Pocock et al., 2008). The construct showed normal localization to the sublateral lines in the hypodermal cell (data not shown), but completely failed to rescue the PVD dendritic phenotype. We thus reason that it is the FnIII domains but not the Ig domains that participate in the tripartite binding. *In vitro* binding experiment with S2 cells showed results consistent with this idea. Cells expressing MNR-1 and SAX-7 without Ig domains could still form large aggregates with DMA-1 expressing cells, while cells co-expressing MNR-1 and SAX-7 without FnIII domains completely failed to do so (Fig. 7D, Fig. S6D, E).

In vivo and *in vitro* experiments together provide evidence that the three proteins form a tripartite complex, with SAX-7 and MNR-1 forming a co-ligand and DMA-1 interacting in *trans*. We thus propose a model in which SAX-7 and MNR-1 form pre-patterned cues in the hypodermal cell and DMA-1 responds to this signal to direct the proper formation and growth of PVD dendrites (Fig. 7F, Fig. S6F).

Discussion

Environmental signals instruct dendrite morphogenesis

The precise spatial patterning of dendritic arbors requires delicate interactions between dendrites and their growing environment. Dendrite surface receptors must sense various types of extrinsic signals: global diffusible factors that determine their general orientation (Polleux et al., 2000), local cell adhesion molecules on the growth substrate that defines their spatial territories (Han et al., 2012; Kim et al., 2012), and signals from other neurites including axon terminals of their presynaptic partners (Sanes and Yamagata, 2009; Yamagata and Sanes, 2012) and dendrites from the same cell and neighboring arbors (Han et al., 2012; Lefebvre et al., 2012; Matthews et al., 2007; Soba et al., 2007).

To extend our molecular knowledge of the interaction between dendrites and their environment, we report the identification of three cell adhesion molecules that form a tripartite receptor-ligand complex between skin hypodermal cells and developing neuronal dendrites. In the hypodermal cell, SAX-7/L1CAM, an Ig cell adhesion molecule, forms a precise subcellular pattern, on which the dendrites later grow. To the best of our knowledge, such a precisely localized patterning signal has not been previously reported for dendrite development. However, there is evidence suggesting the existence of such molecular signals for precise spatial patterning of dendrites. For example, DA neurons in adult *Drosophila* establish a lattice-like morphology along the basement membrane between muscle fibers underneath the epidermis (Yasunaga et al., 2010). Multi-modal somatosensory neurons in vertebrates also establish similar stereotyped rather than random morphologies (Hall and Treinin, 2011). In the mammalian retina, dendritic arbors of amacrine cells and retinal ganglion cells (RGCs) are strictly organized in defined laminae in the inner plexiform layer (IPL) (Sanes and Zipursky, 2010). Time lapse imaging of the zebrafish retina revealed that at least some RGC dendrites elaborate branched arbors only when they reached their target layer, indicating the existence of branch promoting factors arrayed within the IPL (Mumm et al., 2006; Yamagata and Sanes, 2012). Although specific instructive molecules are yet to be identified for these examples, the highly organized morphology and specific branching locations strongly suggest the existence of such extrinsic signals. In our system, the activity of SAX-7 requires another transmembrane protein, MNR-1, which also functions in the hypodermal cell. The cognate neuronal receptor for SAX-7 and MNR-1 is a LRR transmembrane protein, DMA-1, which promotes selective stabilization and further branching of the dendrites at specific locations pre-defined by the SAX-7 and MNR-1 signal. All three molecules have homologues in vertebrate genomes (Fig. S1), supporting the notion that the molecular players as well as the organizing principles in dendrite morphogenesis might be conserved throughout evolution.

A tripartite complex of adhesion molecules

SAX-7/L1CAM has been intensively studied for its functions in maintaining neuronal integrity, axon outgrowth and cell migration (Brummendorf et al., 1998; Pocock et al., 2008; Sasakura et al., 2005; Zallen et al., 1999). Mutations in human L1 have been linked to a number of neurological abnormalities (Van Camp et al., 1996; Vits et al., 1994). Here we report a new function of SAX-7/L1CAM that is likely different from those that have been previously studied. First, rather than functioning as a recognition molecule in the neuron, we found that SAX-7 was expressed and subcellularly localized in the hypodermal cell, the substrate upon which the neuron grows. Second, the function of SAX-7 was exerted under the assistance of another novel transmembrane co-ligand, MNR-1. Third, although all previously reported functions of SAX-7 require homotypic interactions between the Ig domains (Pocock et al., 2008; Schurmann et al., 2001), the binding we report here requires the FnIII domains of SAX-7.

Our genetic analyses suggest that the novel protein MNR-1 functions as the co-ligand of SAX-7 in patterning PVD dendrites. First, *sax-7* and *mnr-1* mutants exhibited indistinguishable phenotypes. Second, both MNR-1 and SAX-7 were expressed and required in the hypodermal cells. Third, the gof activity caused by ectopic expression of SAX-7 and MNR-1 required both molecules. Fourth, SAX-7 only bound to DMA-1 in the presence of MNR-1. The genetic requirement of MNR-1 for SAX-7 gof phenotypes in tissues that did not express MNR-1 suggests that MNR-1 is partially secreted. This hypothesis is supported by the accumulation of fluorescently tagged MNR-1 in coelomocytes. More detailed genetic and protein structure-function analysis will be needed to fully understand MNR-1's functions and mechanisms of its secretion.

As we have previously reported, DMA-1 is a good candidate as the neuronal receptor to regulate the development of dendritic arbors (Liu and Shen, 2012). In this report, we present evidence that DMA-1 functions as the cognate neuronal receptor for SAX-7 and MNR-1. First, *dma-1* mutants exhibited similar phenotypes in 3° branch formation as seen in *sax-7* and *mnr-1* mutants. Second, DMA-1 was absolutely required for the gof phenotypes caused by ectopic expression of SAX-7 and MNR-1, while overexpressing DMA-1 in *sax-7* or *mnr-1* mutants does not alter their PVD dendritic phenotype. Third, DMA-1 bound to the SAX-7/MNR-1 complex *in vitro*. We speculate that the difference in the number of branches formed in these mutants can be explained by the selective loss of adhesion. *dma-1* mutants are lacking adhesion in the dendritic branches themselves, making branch growth and stabilization to any degree difficult (Movie S4). However, in the *sax-7* and *mnr-1* mutants, DMA-1 is still present in the dendritic branches. If DMA-1 can interact at least somewhat with other proteins (perhaps expressed on the surface of the gut or gonad), then in the absence of its preferred substrate (SAX-7/MNR-1), the branches may over-grow in an attempt to find the appropriate signal. In both wild-type animals and gof experiments, DMA-1-containing dendrites contacting with a source of SAX-7 and MNR-1 lead to a universal reduction in undirected branching (Fig. 6B, D, E), suggesting that formation of the tripartite receptor-ligand complex can both reinforce "appropriate" dendritic branch growth while suppressing "inappropriate" growth in other locations.

A model to explain how the tripartite complex patterns dendritic arbors in PVD

Collectively, our results are consistent with the following speculative model to explain the orderly-branched PVD dendrites. The PVD dendritic arbors are established in a sequential manner. 2° branches are formed from the primary dendrite shaft. When the 2° processes encounter the 3° line, the high concentration of SAX-7 and MNR-1 activate DMA-1 on the neurite, possibly leading to both a tighter adhesion and signaling events that recruit cytoskeletal components necessary to form and maintain branches (Fig. 7F, Fig. S6F). The exact mechanisms leading to the decisions of dendrite growth, branching, or retraction in response to extrinsic signals remain to be characterized. However, the identification of surface receptor-ligand interactions opens the door for analysis of the elaborate underlying cellular processes just like those that have now been studied in great detail for axon guidance.

Experimental Procedures

Strains and plasmids

N2 Bristol was used as the wild-type strain. Worms were raised on OP50 *Escherichia coli*-seeded nematode growth medium plates at 20 °C or room temperature, following standard protocol (Brenner, 1974). All transgenes and plasmids are listed in Tables S1 and S2.

Isolation and mapping of *mnr-1(wy758)* mutant

The *wy758* allele was isolated from an F2 semiclonal screen of 3000 haploid genomes in the strain *wyIs378*. Worms were mutagenized with 50 mM EMS. SNIP-SNP mapping, rescue, and sequencing were performed using standard protocols (Matthews et al., 2007). This allele carries a non-sense G-to-A point mutation flanked by sequences TTTAAGGAAT and GCTCAGAGAA.

Time lapse imaging

Worms were raised at approximately 22°C and prepared for imaging as previously described (McCarter et al., 1999). Briefly, worms were soaked in a solution of 0.1% tricaine and 0.01% levamisole (Sigma-Aldrich) in M9 for 20-30 minutes prior to imaging. The immobilized worms were then transferred with a glass hook to a drop of M9 containing 0.05 micron polystyrene microspheres (Polysciences) on a slab of 5% agarose in M9. The coverslip was then sealed with Vaseline. Images were acquired using a Zeiss Axio Observer Z1 microscope equipped with a Plan-Apochromat 63× 1.4 objective (Carl Zeiss), Yokagawa spinning disk head, 488 and 561 diode lasers, and a Hamamatsu ImagEm EMCCD camera driven by MetaMorph (Molecular Devices). To follow dendrite branching, a stack of both GFP and mCherry images with 15 z-planes at 0.5 μm intervals was acquired every 2 min. Maximum intensity projections were created for analysis and presentation. Movies of similarly aged worms imaged just anterior to the cell body were scored for the time points at which branch initiation or retraction occurred to determine initiation and stabilization rates over the course of filming (approximately 2-3 hours). Due to the infrequency of 3° branch initiation in the mutants, a 3° branch was counted as stabilized if it was present at the end of filming, rather than existing for a minimum lifespan.

S2 cell aggregation and co-IP assays

Drosophila S2 cells were cultured in Schneider's insect medium (Sigma) according to the manufacturer's description and transfected using Effectene (Qiagen). S2 cell aggregation assays were performed as previously described (Zorio et al., 1994). All plasmids used for transfection are listed in Table S3. The detailed experimental procedure is included in the Supplemental experimental procedures.

Supplementary Material

Refer to Web version on PubMed Central for supplementary material.

Acknowledgments

This work was supported by the Howard Hughes Medical Institute and by NIH (1R01NS082208-01A1). We thank the Caenorhabditis Genetics Center for the *sax-7(nj48)* strain and the laboratory of H. Beulow for sharing of unpublished information. We also thank C. Yu for helping in forward genetic screens, C. Gao and the laboratories of L. Luo and K. C. Garcia for technical assistance and G. Maro, C. A. Taylor and V. Ericson for thoughtful comments on the manuscript.

References

Aguirre-Chen C, Bülow HE, Kaprielian Z. C. elegans bicd-1, homolog of the Drosophila dynein accessory factor Bicaudal D, regulates the branching of PVD sensory neuron dendrites. Development. 2011; 138:507–518. [PubMed: 21205795]

Albeg A, Smith CJ, Chatzigeorgiou M, Feitelson DG, Hall DH, Schafer WR, Miller DM Iii, Treinin M. C. elegans multi-dendritic sensory neurons: Morphology and function. Molecular and Cellular Neuroscience. 2011; 46:308–317. [PubMed: 20971193]

Brenner S. The genetics of Caenorhabditis elegans. Genetics. 1974; 77:71–94. [PubMed: 4366476]

Brummendorf T, Kenwrick S, Rathjen FG. Neural cell recognition molecule L1: from cell biology to human hereditary brain malformations. Curr Opin Neurobiol. 1998; 8:87–97. [PubMed: 9568396]

Hall DH, Treinin M. How does morphology relate to function in sensory arbors? Trends in Neurosciences. 2011; 34:443–451. [PubMed: 21840610]

Han C, Wang D, Soba P, Zhu S, Lin X, Jan Lily Y, Jan Y-N. Integrins Regulate Repulsion-Mediated Dendritic Patterning of Drosophila Sensory Neurons by Restricting Dendrites in a 2D Space. Neuron. 2012; 73:64–78. [PubMed: 22243747]

Hong W, Zhu H, Potter CJ, Barsh G, Kurusu M, Zinn K, Luo L. Leucine-rich repeat transmembrane proteins instruct discrete dendrite targeting in an olfactory map. Nat Neurosci. 2009; 12:1542–1550. [PubMed: 19915565]

Jan Y-N, Jan LY. Branching out: mechanisms of dendritic arborization. Nat Rev Neurosci. 2010; 11:316–328. [PubMed: 20404840]

Kim, Michelle E.; Shrestha, Brikha R.; Blazeski, R.; Mason, Carol A.; Grueber, Wesley B. Integrins Establish Dendrite-Substrate Relationships that Promote Dendritic Self-Avoidance and Patterning in Drosophila Sensory Neurons. Neuron. 2012; 73:79–91. [PubMed: 22243748]

Komiyama T, Sweeney LB, Schuldiner O, Garcia KC, Luo L. Graded Expression of Semaphorin-1a Cell-Autonomously Directs Dendritic Targeting of Olfactory Projection Neurons. Cell. 2007; 128:399–410. [PubMed: 17254975]

Lefebvre JL, Kostadinov D, Chen WV, Maniatis T, Sanes JR. Protocadherins mediate dendritic self-avoidance in the mammalian nervous system. Nature. 2012; 488:517–521. [PubMed: 22842903]

Liu OW, Shen K. The transmembrane LRR protein DMA-1 promotes dendrite branching and growth in C. elegans. Nat Neurosci. 2012; 15:57–63. [PubMed: 22138642]

Matsuoka RL, Jiang Z, Samuels IS, Nguyen-Ba-Charvet KT, Sun LO, Peachey NS, Chédotal A, Yau K-W, Kolodkin AL. Guidance-Cue Control of Horizontal Cell Morphology, Lamination, and Synapse Formation in the Mammalian Outer Retina. The Journal of Neuroscience. 2012; 32:6859–6868. [PubMed: 22593055]

Matthews BJ, Kim ME, Flanagan JJ, Hattori D, Clemens JC, Zipursky SL, Grueber WB. Dendrite Self-Avoidance Is Controlled by Dscam. Cell. 2007; 129:593–604. [PubMed: 17482551]

McCarter J, Bartlett B, Dang T, Schedl T. On the Control of Oocyte Meiotic Maturation and Ovulation in Caenorhabditis elegans. Developmental Biology. 1999; 205:111–128. [PubMed: 9882501]

Mumm JS, Williams PR, Godinho L, Koerber A, Pittman AJ, Roeser T, Chien C-B, Baier H, Wong ROL. In Vivo Imaging Reveals Dendritic Targeting of Laminated Afferents by Zebrafish Retinal Ganglion Cells. Neuron. 2006; 52:609–621. [PubMed: 17114046]

Oren-Suissa M, Hall DH, Treinin M, Shemer G, Podbilewicz B. The Fusogen EFF-1 Controls Sculpting of Mechanosensory Dendrites. Science. 2010; 328:1285–1288. [PubMed: 20448153]

Pocock R, Bénard CY, Shapiro L, Hobert O. Functional dissection of the C. elegans cell adhesion molecule SAX-7, a homologue of human L1. Molecular and Cellular Neuroscience. 2008; 37:56–68. [PubMed: 17933550]

Polleux F, Morrow T, Ghosh A. Semaphorin 3A is a chemoattractant for cortical apical dendrites. Nature. 2000; 404:567–573. [PubMed: 10766232]

Sanes JR, Yamagata M. Many Paths to Synaptic Specificity. Annual Review of Cell and Developmental Biology. 2009; 25:161–195.

Sanes JR, Zipursky SL. Design Principles of Insect and Vertebrate Visual Systems. Neuron. 2010; 66:15–36. [PubMed: 20399726]

Sasakura H, Inada H, Kuhara A, Fusaoka E, Takemoto D, Takeuchi K, Mori I. Maintenance of neuronal positions in organized ganglia by SAX-7, a Caenorhabditis elegans homologue of L1. EMBO J. 2005; 24:1477–1488. [PubMed: 15775964]

Schmucker D, Clemens JC, Shu H, Worby CA, Xiao J, Muda M, Dixon JE, Zipursky SL. Drosophila Dscam Is an Axon Guidance Receptor Exhibiting Extraordinary Molecular Diversity. Cell. 2000; 101:671–684. [PubMed: 10892653]

Schurmann G, Haspel J, Grumet M, Erickson HP. Cell adhesion molecule L1 in folded (horseshoe) and extended conformations. Mol Biol Cell. 2001; 12:1765–1773. [PubMed: 11408583]

Smith, Cody J.; O Brien, T.; Chatzigeorgiou, M.; Spencer, WC.; Feingold-Link, E.; Husson, Steven J.; Hori, S.; Mitani, S.; Gottschalk, A.; Schafer, William R., et al. Sensory Neuron Fates Are

Distinguished by a Transcriptional Switch that Regulates Dendrite Branch Stabilization. Neuron. 2013; 79:266–280. [PubMed: 23889932]

Smith CJ, Watson JD, Spencer WC, O'Brien T, Cha B, Albeg A, Treinin M, Miller DM Iii. Time-lapse imaging and cell-specific expression profiling reveal dynamic branching and molecular determinants of a multi-dendritic nociceptor in C. elegans. Developmental Biology. 2010; 345:18–33. [PubMed: 20537990]

Smith CJ, Watson JD, VanHoven MK, Colon-Ramos DA, Miller DM. Netrin (UNC-6) mediates dendritic self-avoidance. Nat Neurosci. 2012; 15:731–737. [PubMed: 22426253]

Soba P, Zhu S, Emoto K, Younger S, Yang S-J, Yu H-H, Lee T, Jan LY, Jan Y-N. Drosophila Sensory Neurons Require Dscam for Dendritic Self-Avoidance and Proper Dendritic Field Organization. Neuron. 2007; 54:403–416. [PubMed: 17481394]

Sulston JE, Horvitz HR. Post-embryonic cell lineages of the nematode, Caenorhabditis elegans. Developmental Biology. 1977; 56:110–156. [PubMed: 838129]

Tursun B, Cochella L, Carrera I, Hobert O. A Toolkit and Robust Pipeline for the Generation of Fosmid-Based Reporter Genes in *C. elegans*. PLoS ONE. 2009; 4:e4625. [PubMed: 19259264]

Van Camp G, Fransen E, Vits L, Raes G, Willems PJ. A locus-specific mutation database for the neural cell adhesion molecule L1CAM (Xq28). Hum Mutat. 1996; 8:391. [PubMed: 8956051]

Vits L, Van Camp G, Coucke P, Fransen E, De Boulle K, Reyniers E, Korn B, Poustka A, Wilson G, Schrander-Stumpel C, et al. MASA syndrome is due to mutations in the neural cell adhesion gene L1CAM. Nat Genet. 1994; 7:408–413. [PubMed: 7920660]

Wojtowicz WM, Flanagan JJ, Millard SS, Zipursky SL, Clemens JC. Alternative Splicing of Drosophila Dscam Generates Axon Guidance Receptors that Exhibit Isoform-Specific Homophilic Binding. Cell. 2004; 118:619–633. [PubMed: 15339666]

Wojtowicz WM, Wu W, Andre I, Qian B, Baker D, Zipursky SL. A Vast Repertoire of Dscam Binding Specificities Arises from Modular Interactions of Variable Ig Domains. Cell. 2007; 130:1134–1145. [PubMed: 17889655]

Yamagata M, Sanes JR. Dscam and Sidekick proteins direct lamina-specific synaptic connections in vertebrate retina. Nature. 2008; 451:465–469. [PubMed: 18216854]

Yamagata M, Sanes JR. Expanding the Ig Superfamily Code for Laminar Specificity in Retina: Expression and Role of Contactins. The Journal of Neuroscience. 2012; 32:14402–14414. [PubMed: 23055510]

Yasunaga, K-i; Kanamori, T.; Morikawa, R.; Suzuki, E.; Emoto, K. Dendrite Reshaping of Adult Drosophila Sensory Neurons Requires Matrix Metalloproteinase-Mediated Modification of the Basement Membranes. Developmental Cell. 2010; 18:621–632. [PubMed: 20412776]

Zallen JA, Kirch SA, Bargmann CI. Genes required for axon pathfinding and extension in the C. elegans nerve ring. Development. 1999; 126:3679–3692. [PubMed: 10409513]

Zorio DAR, Cheng NN, Blumenthal T, Spieth J. Operons as a common form of chromosomal organization in C. elegans. Nature. 1994; 372:270–272. [PubMed: 7969472]

Highlights

- SAX-7/L1CAM acts as a spatially patterned guidance cue in the hypodermis.
- SAX-7/L1CAM and MNR-1 guide the outgrowth, branching and stability of dendrites.
- DMA-1 acts as the neuronal receptor for SAX-7 and MNR-1.

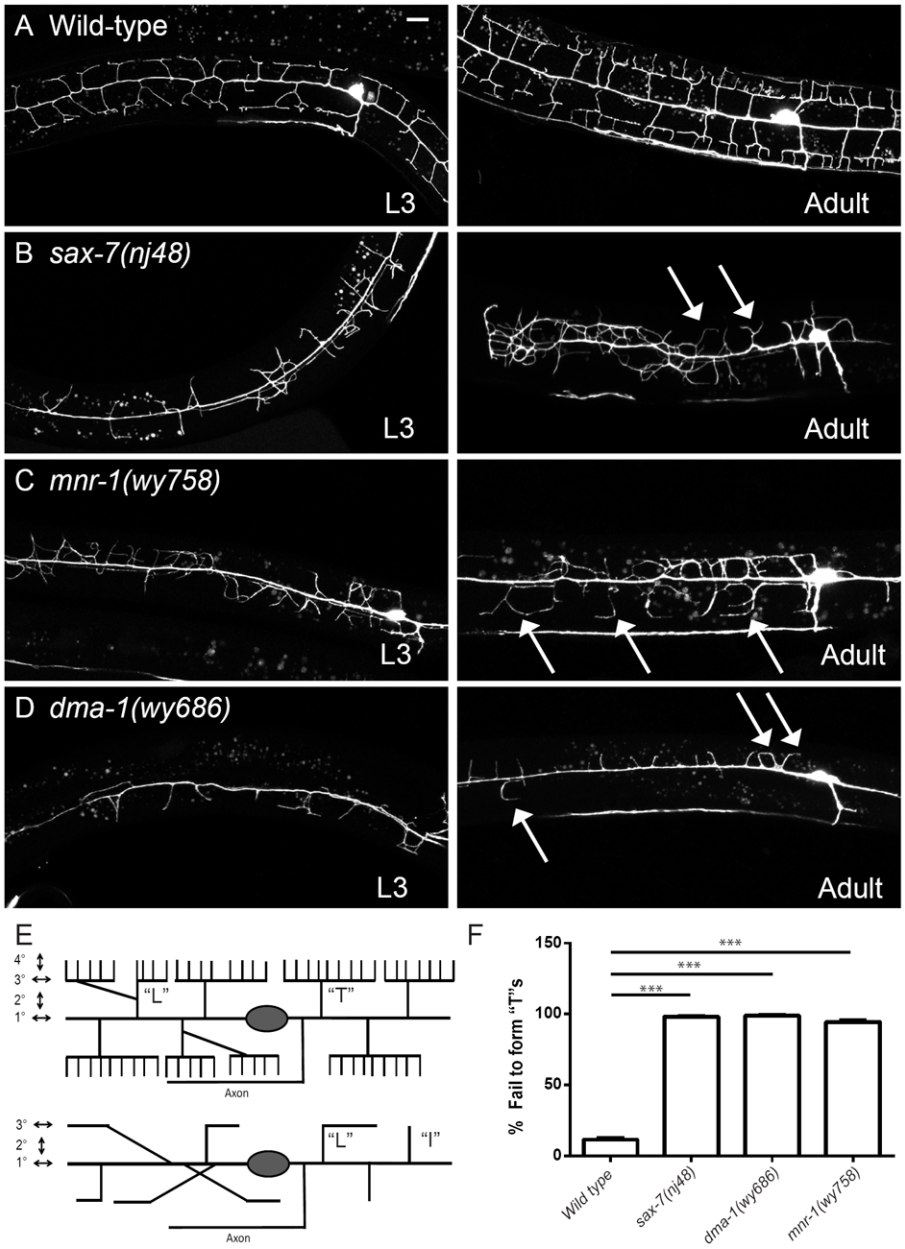

Figure 1. *sax-7, mnr-1 and dma-1* mutants showed severe defects in PVD morphology

(A-E). Confocal images showing PVD morphology of wild-type (A), *sax-7(nj48)* (B), *mnr-1(wy758)* (C), and *dma-1(wy686)*(D) mutant worms at the L3 stage (left row), or adult stage (right row). PVD morphology was visualized by a cell-specific fluorescent marker (*wyIs378*). Arrows: Branches that turn and form "L"s but fail to branch and form "T"s at the 3° line. Scale bar: 10 μM. (E) Schematic of PVD dendrite morphology in wild-type and mutant worms. "T"s: Dendrites that extended in both directions along the 3° line. "L"s: Dendrites that turned at the 3° line but failed to form a collateral branch. "I"s: Dendrites that reached the 3° line but failed to either bifurcate or turn. (F) Quantification of the % of dendrites per worm that reached the 3° line but failed to form "T"s. Error bars: Standard error of the mean. *** is $p<0.001$ by Student's T-test. N=50 for each genotype. See also Figure S1.

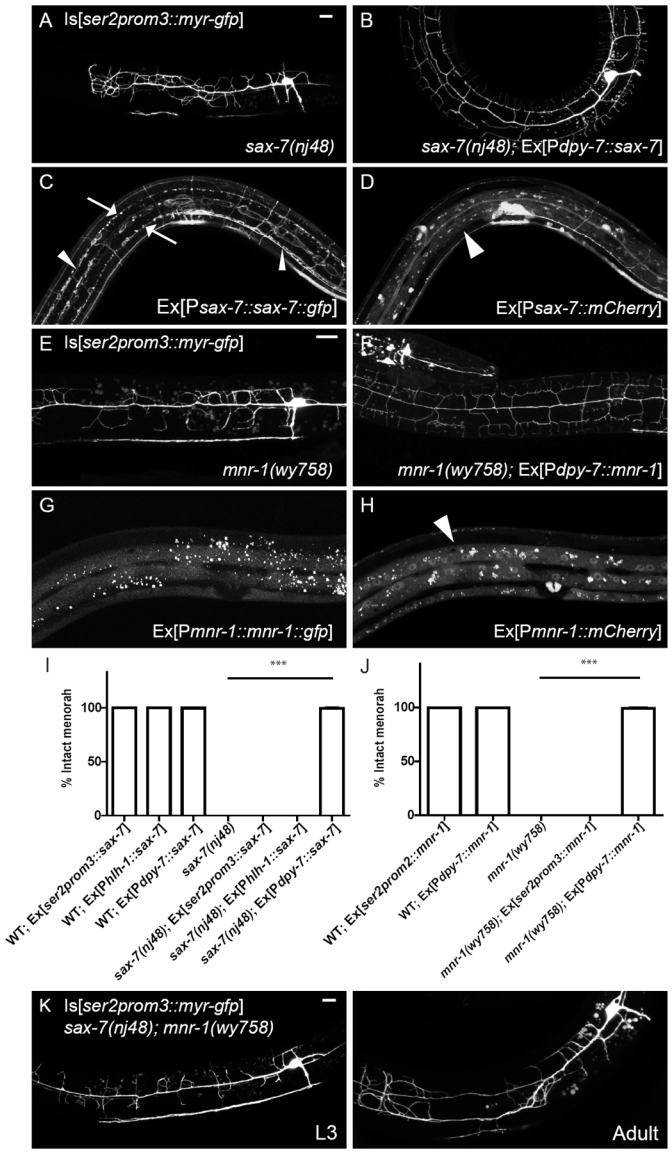

Figure 2. SAX-7 and MNR-1 functioned in the hypodermal cell

(A). *sax-7(nj48)* mutants had severely defective PVD morphology. (B) The mutant phenotype could be fully rescued by expressing SAX-7 in the hypodermal cells using the *dpy-7* promoter. (C, D) SAX-7 was expressed in neurons and the hypodermal cells (D) and localized subcellularly to two lateral stripes in the hypodermal cell (C). (E, F) The PVD morphology defects in *mnr-1(wy758)* (E) were also fully rescued by expressing MNR-1 in the hypodermal cell using the *dpy-7* promoter (F). (G, H) MNR-1 was only expressed in the hypodermis (H) and showed no obvious subcellular localization (G). (I) Expression of SAX-7 in hypodermal cells rescued the mutant phenotype in all transgenic animals, whereas no rescue was observed when SAX-7 was expressed in the PVD neuron using the *ser2prom3* promoter, or in the muscles using the *myo-2* promoter. (J) Expression of MNR-1 in the hypodermal cells also rescued the *mnr-1(wy758)* mutant phenotype, while expression in PVD using the *ser2prom3* promoter failed to rescue. (K) PVD morphology in *sax-7(nj48); mnr-1(wy758)* double mutants was indistinguishable from the single mutants. Arrows in (C): SAX-7 sublateral stripes in hypodermal cells. Arrowheads in (C): SAX-7

expressed in the ALM and PLM neurons. Arrow head in (D) and (H): Fluorescent labeling of the hypodermal cells. Scale bar: 10 μm. Error bars: Standard error of the mean. *** is $p<0.001$ by student's T-test. N=20 for all genotypes. See also Figure S2.

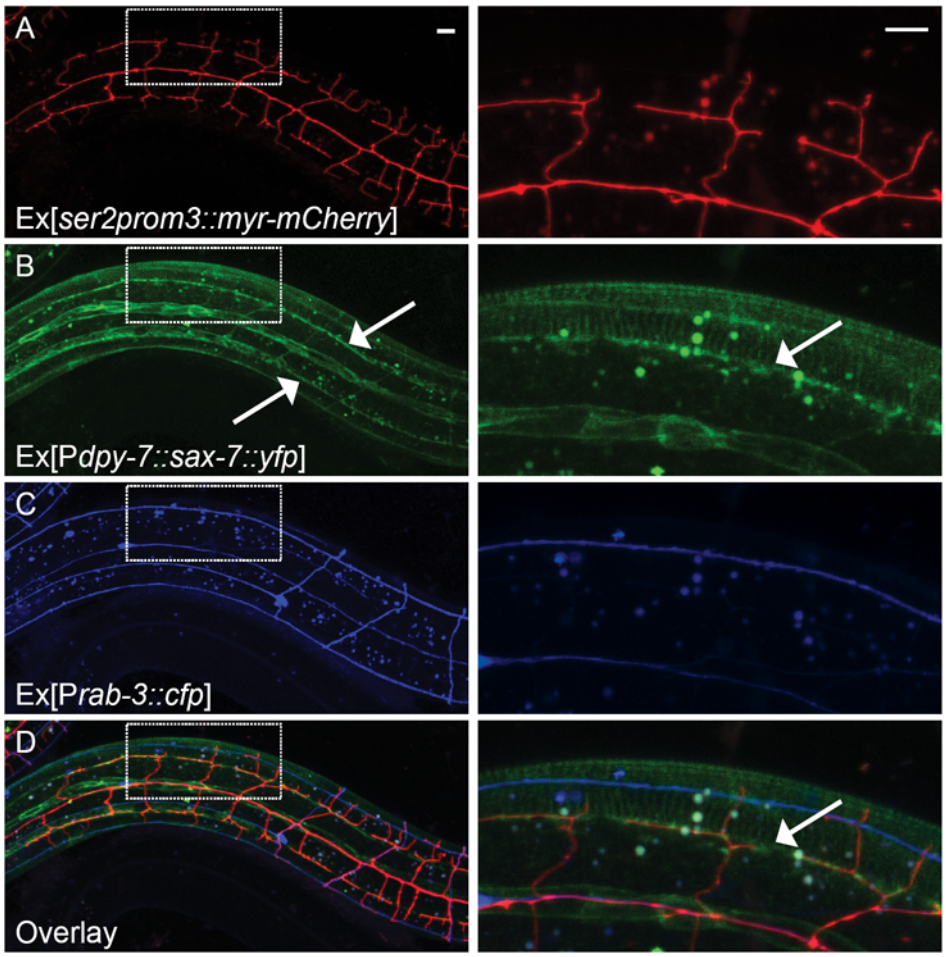

Figure 3. SAX-7 was enriched in sublateral stripes in the hypodermis

(A-D) Fluorescent images showing (A) PVD neuron, (B) SAX-7 localization, (C) all neurons and (D) overlay of the three colors. SAX-7 was localized to 2 sublateral longitudinal lines in the hypodermal cells on each side of the worm. PVD 3° branches completely co-localized with the SAX-7 lines but did not fasciculate with any other neurons in the anterior part of the worm. Arrows: Sublateral stripes of enriched SAX-7 that co-localize with PVD 3° dendrites. The images on the right are zoomed-in views of the region indicated by the box. Scale bar: 10 μm. See also Figure S2.

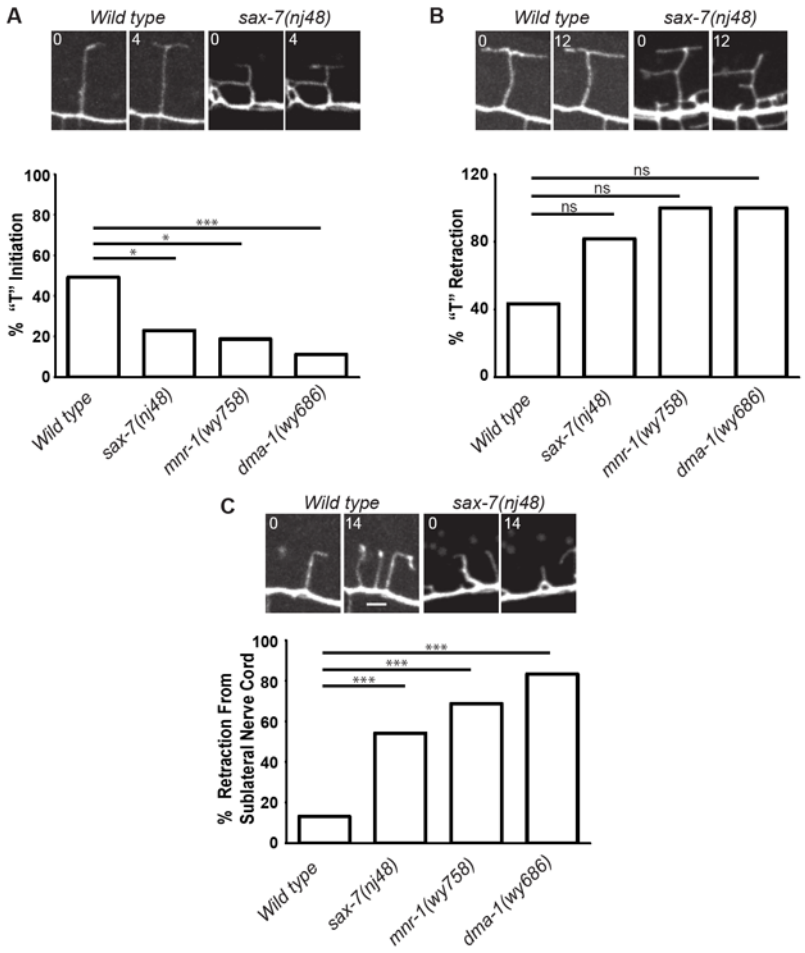

Figure 4. Branching defects in *sax-7*, *mnr-1*, and *dma-1* mutants were due to decreased branch initiation and stability

(A) The percentage of dendritic branches that initiated a "T" following arrival at the 3° line, as determined by the pan-neuronal mCherry signal. (B) The percentage of branches that retracted a "T" after formation. (C) The percentage of branches that reached the 3° line that subsequently retracted away from the 3° line, towards the 1° dendrite. * is $p<0.0083$, ** is $p<0.0017$, *** is $p<0.00017$, n.s. : non-significant by Fisher's exact test with Bonferroni correction. There were no statistically significant differences between the mutants. Time is in min. Examples of branch behavior are shown in pictures at the top of each panel. Scale bar: 2μm. See also Movies S1-S4.

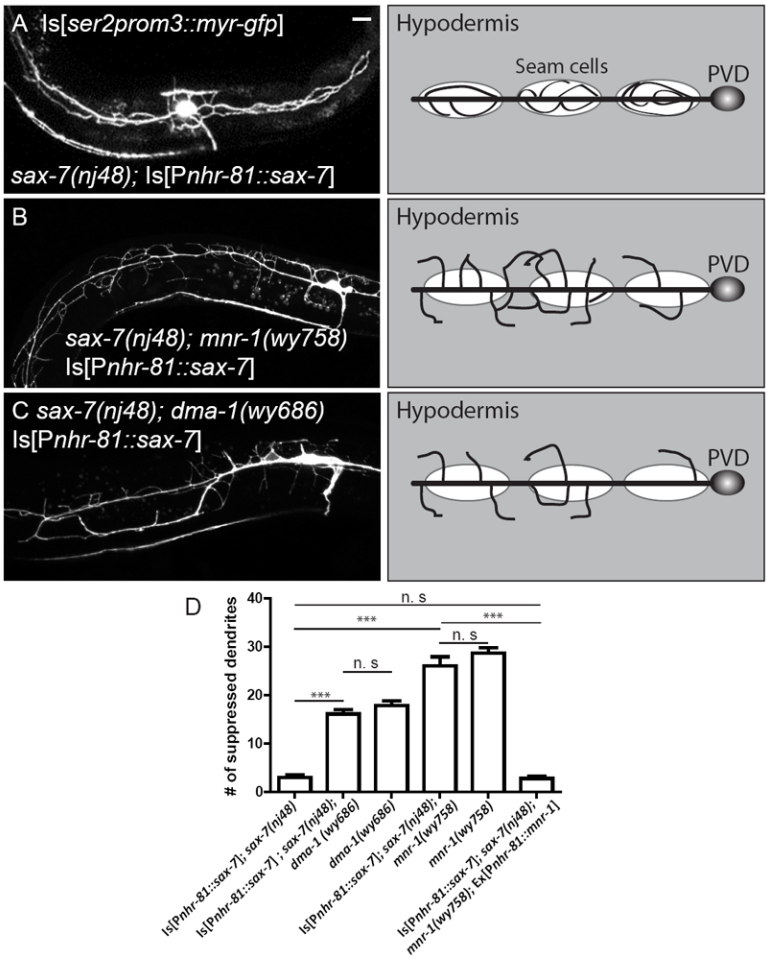

Figure 5. Ectopic expression of SAX-7 in seam cells caused a dramatic gain of function (gof) phenotype

(A) Ectopic expression of SAX-7 in the seam cells in *sax-7(nj48)* mutant worms caused the dendrites to be restricted around the seam cells instead of growing towards the dorsal and ventral midlines (*wyIs369*). (B) *mnr-1(wy758)* fully suppressed the gof phenotype. PVD morphology was identical to that of *mnr-1(wy758)* mutants without the *wyIs369* transgene. (C) *dma-1(wy686)* fully suppressed the gof phenotype generated by overexpressing SAX-7 in seam cells. PVD morphology was identical to that of *dma-1(wy686)* mutants without the *wyIs369* transgene. (D). Quantification of the number of dendrites per worm that protrude outside the estimated area covered by the seam cells. Error bars: Standard error of the mean. *** is $p<0.001$, n.s. is non-significant by Student's T-test. Scale bar: 10 μm. N=50 for each genotype. See also Figure S3.

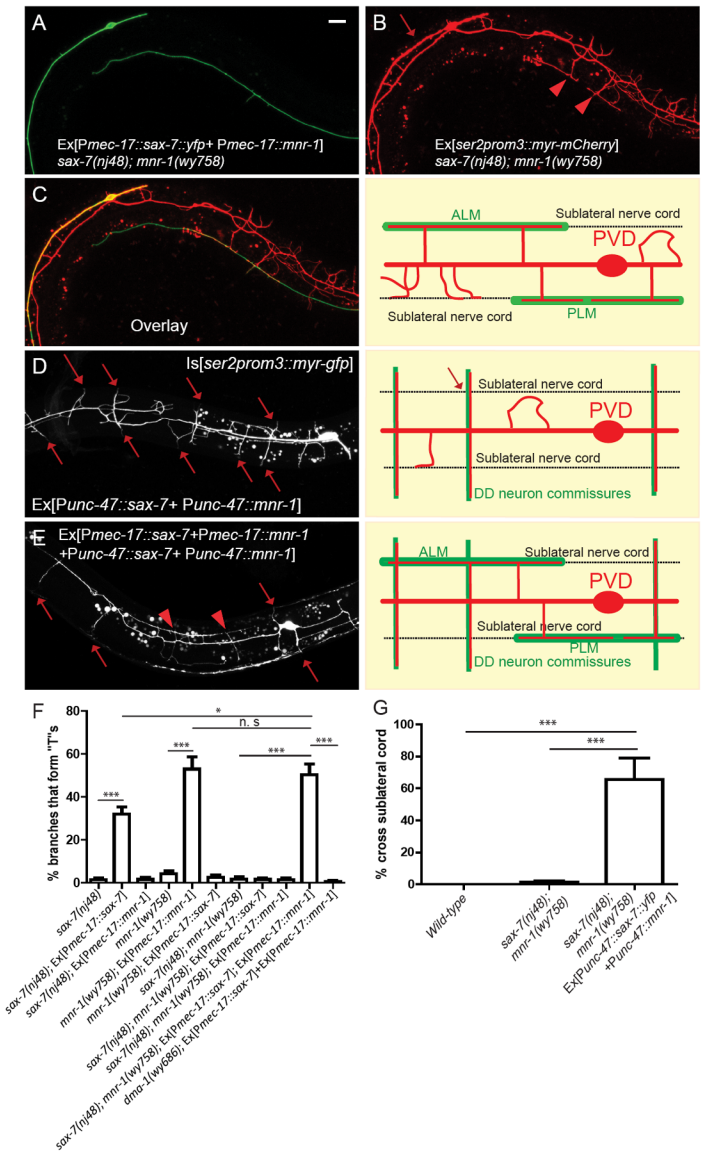

Figure 6. Expression of SAX-7 and MNR-1 in other neurons was sufficient to modify PVD morphology

(A) Fluorescent image showing PLM and ALM neurons expressing SAX-7 and MNR-1 (B) The 3° branching defect in *sax-7; mnr-1* double mutants could be partially rescued by expressing SAX-7 and MNR-1 in PLM and ALM. Arrowheads: PVD branches that formed "T"s when they reached the PLM neuron expressing SAX-7 and MNR-1. Arrow: PVD process completely followed the ALM neuron expressing SAX-7 and MNR-1. (C) Left: Overlay between (A) and (B). Right: Schematic illustration of the phenotype. (D) Ectopic expression of SAX-7 and MNR-1 in DD motor neuron commissures caused the branches to grow symmetrically towards both the dorsal and ventral sides and cross the sublateral nerve cord where they would normally turn and form 3° branches. Arrows: PVD 2° branches that cross the sublateral nerve cords. (E) Ectopic expression of SAX-7 and MNR-1 in PLM, ALM, and DD neurons reshaped the PVD dendritic morphology. (F) Quantification of the percentage of branches per worm that made contact with the SAX-7 and MNR-1 expressing PLM or ALM neurons and formed "T"s. (G) Quantification of the percentage of 2° branches per worm that crossed the sublateral nerve cord. Error bars: Standard error of the mean. ***

is $p<0.001$ by Student's T-test. Scale bar: 10 μm. N=20 for all genotypes. See also Figure S4 and S5.

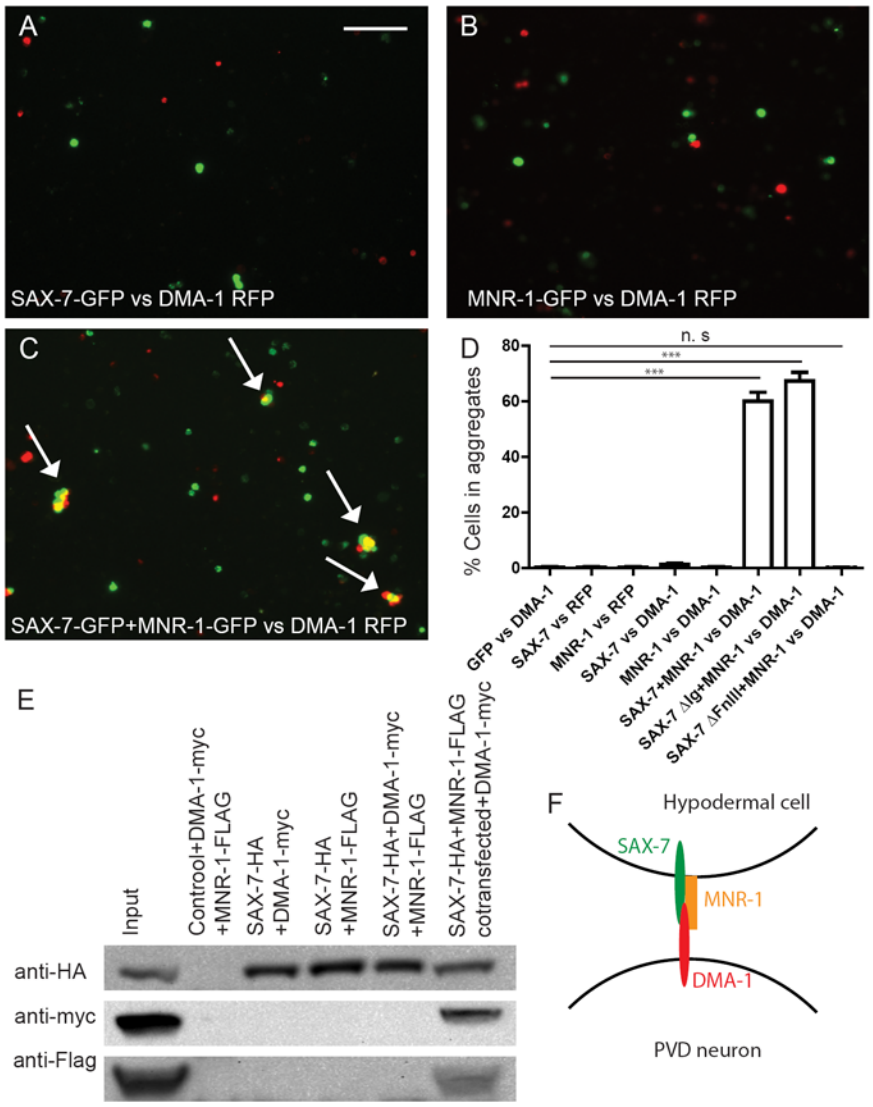

Figure 7. DMA-1 physically interacted with SAX-7 and MNR-1

Drosophila S2 cells transfected with only *sax-7∷gfp* (A) or *mnr-1∷gfp* (B) did not aggregate with cells expressing DMA-1-RFP. (C) Cells transfected with both *sax-7∷gfp* and *mnr-1∷gfp* strongly aggregated with cells expressing DMA-1-RFP. Arrows: Aggregates with both green and red transfected cells. (D). Quantification of the percentage of cells in aggregates. Error bars: Standard error of the mean. *** is $p<0.001$ by Student's T-test. Scale bar: 100 μm. (E) Co-immunoprecipitation of HA-tagged SAX-7, Myc-tagged DMA-1 ecto domain and FLAG-tagged MNR-1. (F) Schematic model of a tripartite complex. SAX-7 and MNR-1 form a co-ligand complex on the hypodermal cells and instructs dendrite morphogenesis through binding to DMA-1 on the neuron. See also Figure S6.